

# Low-Temperature Vapor–Liquid Equilibria from Parallelized Molecular Dynamics Simulations. Application to 1- and 2-Methylnaphthalene

Martin Lísal,<sup>†,‡</sup> Ivo Nezbeda,<sup>\*,†,§</sup> Philippe Ungerer,<sup>||</sup> Jean-Marie Teuler,<sup>⊥</sup> and Bernard Rousseau<sup>⊥</sup>

*E. Hála Laboratory of Thermodynamics, Institute of Chemical Process Fundamentals, Academy of Sciences of the Czech Republic, 165 02 Prague 6-Suchbát, Czech Republic, Department of Physics, J. E. Purkinje University, 400 96 Ústí. Lab., Czech Republic, Department of Chemistry, J. E. Purkinje University, 400 96 Ústí. Lab., Czech Republic, Institut Français du Pétrole, 1-4 Av. de Bois Préau, 92852 Reuil-Malmaison Cedex, France, and Department of Physical Chemistry, UMR 8611 CNRS, Université de Paris Sud, bât. 490, 91405 Orsay Cedex, France*

Received: January 17, 2006; In Final Form: April 28, 2006

A parallelized sampling version of the Gibbs Ensemble (*Mol. Phys.* **2000**, 98, 1887) has been implemented to predict low-temperature vapor–liquid equilibria of 1- and 2-methylnaphthalene modeled by anisotropic united atom potentials. The simulation was performed at the low temperature of 364.2 K at which common direct simulation methods fail due to particle transfer problems. The simulation results are compared with published results obtained from the Gibbs–Duhem integration method and with experimental data. Both methods are compared and discussed in terms of computational efficiency and with respect to their future use at other thermodynamic conditions.

## 1. Introduction

Since its invention in 1987,<sup>1</sup> the use of the Gibbs ensemble (GE) has become the most common way to determine vapor–liquid equilibria (VLE) in fluid systems without explicitly considering the interface.<sup>2</sup> For relatively simple, not too dense systems made up of (nearly) spherical molecules and away from the critical point, this type of simulation poses no problems, which, however, are encountered when dealing with, for instance, very dense systems, systems of highly nonspherical molecules, or mixtures of very different components. These problems are directly associated with the exchange of molecules (their insertion and/or deletion) between simulation boxes, which is the necessary step to reach phase equilibrium. Numerous attempts have therefore been made to facilitate the transfer of particles and to make this step more efficient. Most common of these are the expanded-ensemble (fluctuating particle) method,<sup>3,4</sup> thermodynamic integration (TI) ( $\lambda$ -coupling) methods,<sup>5</sup> and free-energy perturbation methods for the evaluation of the excess chemical potential.<sup>6,7</sup> The TI methods and the free-energy perturbation methods are, in a way, equivalent methods, and the expanded-ensemble method requires certain prior knowledge of the balancing factors that are not, in general, easy to determine.

The above-mentioned problems and limitations have severe implications for process engineering applications that involve, typically, compounds of high molecular weight and, hence, also of high boiling temperature. For these compounds, many isomers

exist, but experimental data are, in general, available for a few of them only. Furthermore, a common obstacle for carrying out laboratory experiments is their commercial unavailability. Molecular simulations become then a privileged (and only available) technique to investigate their property/structure relationships.

There is also another problem associated with the GE simulation, namely, that in its original formulation, it does not make it possible to run the simulation in a parallel mode and thus make use of advanced computer technology. Parallelizing the Monte Carlo moves involved in GE calculations is possible to some extent,<sup>8,9</sup> but it is insufficient to compensate for the very low success ratio of transfer moves at temperatures much lower than the normal boiling point. Another possible way to parallelize VLE calculations is to use histogram reweighting methods,<sup>10–12</sup> but their application to low temperatures involves the calculation of numerous state points up to near-critical temperatures. The same applies to the Gibbs–Duhem integration (GDI) method.<sup>13</sup> Another possible way to parallelize the GE simulation was apparently first mentioned by Shing and Azadipour,<sup>14</sup> who envisaged an extension of a variant of the grand-canonical ensemble simulation in which, instead of the standard attempts to add or remove a real particle according to the instantaneous grand canonical probabilities, one considers transitions between the corresponding canonical subensembles constituting the grand-canonical ensemble.<sup>15</sup> Their idea was then exploited by Strnad and Nezbeda,<sup>16</sup> who reformulated the GE simulation in a such way that the simulation may be split rigorously into a number of completely independent simulations, each representing the simulation of a canonical subensemble with the fixed number of particles in boxes; a collection of such subensembles constitutes then the complete GE. The problem of determination of phase equilibria is thus transformed into the problem of determining the chemical potential in an NVT

\* Corresponding author. E-mail: IvoNez@icpf.cas.cz.

<sup>†</sup> E. Hála Laboratory of Thermodynamics, Institute of Chemical Process Fundamentals.

<sup>‡</sup> Department of Physics, J. E. Purkinje University.

<sup>§</sup> Department of Chemistry, J. E. Purkinje University.

<sup>||</sup> Institut Français du Pétrole.

<sup>⊥</sup> Department of Physical Chemistry, UMR 8611 CNRS, Université de Paris Sud.

ensemble for which a number of sophisticated methods is available. To demonstrate correctness of the proposed method, which is suitable for both Monte Carlo and molecular dynamics, and its equivalence with the standard GE, the parallelized version of the GE (PGE) method was implemented for the square-well fluid. However, we are not aware of any other application of the PGE.

In this paper, we consider an application of the PGE to real compounds, 1- and 2-methylnaphthalene, which are representative of the problems raised by chemical engineering applications: in a recent paper,<sup>17</sup> Ahunbay et al. used GE simulations to determine VLE properties of these compounds, but the method ceased working with decreasing temperature. To trace VLE further to lower temperatures, they had to switch to the GDI method. (We recall that, according to the authors, notation used in Table 5 of the paper<sup>17</sup> is misleading because the data referred to by label  $N$  were actually obtained by the GDI.) In the perspective of a property prediction for alkyl-substituted polyaromatics, it is also important to check that the influence of the position of alkyl substituents is correctly captured with available intermolecular potentials and molecular simulation algorithms. In this respect, 1- and 2-methylnaphthalene display sufficiently high boiling points that they allow a significant test of molecular methods when it comes to the determination of low vapor pressures. The following sections of the paper are organized as follows. The simulation methodology is described in Section 2. Section 3 presents the potential model along with computational details. Results are discussed in Section 4, and Section 5 summarizes conclusions.

## 2. Method

In the conventional GE simulations for a pure fluid, one considers two boxes, each representing a sample of one phase far from the interface, and three types of moves: (1) a random displacement, (2) a random change of volumes, and (3) the transfer of a particle from one box to another. The two boxes together constitute an NVT-like ensemble, which means that the total number of particles,  $N = N_1 + N_2$ , and the total volume of the boxes,  $V = V_1 + V_2$ , are conserved. The partition function of the GE for a one-component system is given<sup>5</sup> by

$$Q_{\text{GE}} = \sum_{N_1=0}^N Q_{N_1, N_2} \quad (1)$$

where  $Q_{N_1, N_2}$  stands for the partition function of the NVT-like subensemble with the fixed distribution of particles in both boxes. Because of the transfer of particles between the boxes, running the GE simulation actually means to “visit” during the simulation NVT-like subensembles with a different distribution of particles. The idea behind the PGE is to consider a set of pairs of boxes, each representing the NVT-like subensemble, and to circumvent the direct transfer (visits of different subensembles) by gathering certain pieces of information from the NVT simulations on these pairs of boxes. A possibility to run the simulation in this truly parallel manner stems from the expression for the ensemble average of an arbitrary quantity  $X$

$$\langle X \rangle_{\text{GE}} = \sum_{N_1=0}^N P_{N_1, N_2} \langle X \rangle_{N_1, N_2} \quad (2)$$

where the probability distribution  $P_{N_1, N_2}$  is related to the partition function  $Q_{N_1, N_2}$  by

$$P_{N_1, N_2} = Q_{N_1, N_2} / Q_{\text{GE}} \quad (3)$$

and  $\langle \dots \rangle_{N_1, N_2}$  denotes the subensemble average.

The key quantity for an implementation of the PGE method is thus the distribution  $P_{N_1, N_2}$ , which can be determined from the NVT-like subensemble simulations from (for details see ref 16)

$$P_{N_1, N_2} = P_{0, N} \frac{\prod_{n_1=0}^{N_1-1} \left\langle \frac{V_1}{n_1 + 1} \exp(-\beta\psi_1) \right\rangle_{n_1, n_2}}{\prod_{n_2=N_2}^{N-1} \left\langle \frac{V_2}{n_2 + 1} \exp(-\beta\psi_2) \right\rangle_{n_1, n_2}} \quad (4)$$

where the reference quantity  $P_{0, N}$  is, due to the condition of normalization  $\sum P_{N_1, N_2} = 1$ , determined unambiguously. In eq 4,  $\beta = 1/(kT)$ ,  $k$  is Boltzmann's constant,  $T$  is the temperature, and  $\psi_i = U_i(N_i + 1) - U_i(N_i)$  is the interaction energy of an additional (ghost) particle with all real particles, and  $U_i$  is the configurational energy.

Equation 4 is exact and was used as is in the original paper.<sup>16</sup> For the purpose of implementation of the PGE method, it may be however simplified in the following way. The quantity  $\langle V_i / (n_i + 1) \exp(-\beta\psi_i) \rangle_{n_1, n_2}$  is related to the chemical potential  $\mu_i$  of the individual boxes in the corresponding NVT-like subensembles<sup>16</sup> via the relation

$$\left\langle \frac{V_i}{n_i + 1} \exp(-\beta\psi_i) \right\rangle_{n_1, n_2} = \exp[-\beta(\mu_i - \mu^0)] \quad (5)$$

where  $\mu^0$  is the standard-state chemical potential of a pure fluid that depends only on  $T$ .  $\mu_i$  can also be calculated as the chemical potential in a canonical ensemble from ref 18

$$\beta(\mu_i - \mu^0) = \ln \frac{N_i + 1}{V_i} - \ln \langle \exp(-\beta\psi_i) \rangle \quad (6)$$

In eq 6,  $\langle \exp(-\beta\psi_i) \rangle$  is related to the excess chemical potential  $\mu^{\text{ex}}(V_i, n_i)$  of a canonical ensemble via the relation

$$\langle \exp(-\beta\psi_i) \rangle = \exp[-\beta\mu^{\text{ex}}(V_i, n_i)] \quad (7)$$

Smit and Frenkel<sup>19</sup> showed that the values of the chemical potentials calculated from eqs 5 and 6 typically differ by less than simulation uncertainty. Thus, using eqs 5–7, eq 4 can be rewritten as

$$P_{N_1, N_2} = P_{0, N} \frac{\prod_{n_1=0}^{N_1-1} \frac{V_1}{n_1 + 1} \exp[-\beta\mu^{\text{ex}}(V_1, n_1)]}{\prod_{n_2=N_2}^{N-1} \frac{V_2}{n_2 + 1} \exp[-\beta\mu^{\text{ex}}(V_2, n_2)]} \quad (8)$$

Practical implementation of the PGE, as suggested by eq 8, relies on two series of  $n_1 V_1 T$  and  $n_2 V_2 T$  simulations in which  $V_1$  and  $V_2$  are fixed, and  $n_1$  and  $n_2 \equiv N - 1 - n_1$  are varied to explore state points in vicinity of a coexistence point. Simulated values of  $\beta\mu^{\text{ex}}(V_i, n_i)$  and the excess internal energy  $U_i^{\text{ex}}$  from these  $n_i V_i T$  simulations, along with the input density  $\rho_i$ ,  $\rho_i = n_i / V_i$ , are used to construct  $P_{N_1, N_2}$  using eq 8 and then to evaluate the coexistence properties using eq 2. Because eq 2 directly leads to coexistence properties, the equality of pressures between

the vapor and liquid phases is automatically satisfied. Note that such an implementation of the PGE differs from that in the original paper,<sup>16</sup> where the volumes of the boxes were allowed to fluctuate. Implementation of the PGE based on eq 8 is more suitable for cases where one phase is treated using a macroscopic thermodynamic model or where methods for evaluation of  $\beta\mu^{\text{ex}}$  require constant volume simulations.

Whereas  $\beta\mu^{\text{ex}}$  of the vapor phase is, with respect to the low-temperature considered, evaluated using a virial equation of state, for determination of  $\beta\mu^{\text{ex}}$  of the liquid-phase, we used the TI ( $\lambda$ -coupling) method.<sup>5</sup> We mention in passing that test runs using single-particle TI were also performed, but they yielded less accurate results than “all-particle” TI ( $\lambda$ -coupling), and because of the size of the molecules, they exhibited also rather a strong system size dependence.

The TI technique relies on a series of canonical simulations for systems with different coupling (scaling) parameter  $\lambda$  that controls interactions between the particles of the system:  $\lambda = 0$  corresponds to a system without any interaction between the particles (ideal-gas limit), and  $\lambda = 1$  corresponds to the system of interest, i.e., the system with all interactions fully switched on. At each canonical simulation, the  $\langle \partial U(\lambda) / \partial \lambda \rangle_\lambda$  is evaluated and then used to determine the excess Helmholtz energy per particle,  $f^{\text{ex}}$ , via the relation<sup>5</sup>

$$f^{\text{ex}} = \frac{1}{N} \int_0^1 \left\langle \frac{\partial U(\lambda)}{\partial \lambda} \right\rangle_\lambda d\lambda \quad (9)$$

Subsequently, the liquid excess chemical potential is computed from

$$\beta\mu^{\text{ex}} = \beta f^{\text{ex}} + \left( \frac{PV}{NkT} - 1 \right) \quad (10)$$

At low temperatures, the vapor phase can be accurately described by a truncated virial equation of state (B-EOS)<sup>20</sup>

$$\frac{PV}{NkT} = 1 + \frac{B}{V} \quad (11)$$

Provided that the second virial coefficient,  $B$ , is known, the gas phase need not be considered explicitly because its properties can be determined from eq 11 and

$$\beta\mu^{\text{ex}}(V, T) = \frac{B}{V} \left( 1 + \frac{B}{V} \right) + \ln \left( 1 + \frac{B}{V} \right) \quad (12)$$

$$\frac{U^{\text{ex}}}{NkT} = -\frac{T}{V} \frac{dB}{dT}$$

### 3. Potential Model and Computational Details

Following our previous study,<sup>17</sup> where it was shown that the properties of 1- and 2-methylnaphthalene were quite accurately described by means of an anisotropic united atom (AUA) potential, we also use these potentials in the present study. The molecules are schematically shown in Figure 1. The AUA model treats  $\text{CH}_3$ ,  $\text{CH}_2$ , and  $\text{CH}$  groups as united atoms with the force centers shifted toward hydrogens. Interaction between the force centers are represented by the Lennard-Jones (LJ) potential. The LJ parameters are derived from ethane,  $n$ -pentane, and  $n$ -dodecane in the case of the  $\text{CH}_3$  group,<sup>21</sup> from benzene in the case of the aromatic  $\text{CH}$  group,<sup>22</sup> and from naphthalene in the case of the aromatic  $\text{C}$  group.<sup>17</sup> The LJ potential parameters along with the molecular geometry are summarized in Table 1. Both molecules are considered planar and rigid. The unlike LJ potential parameters are evaluated using the Lorentz–Berthelot

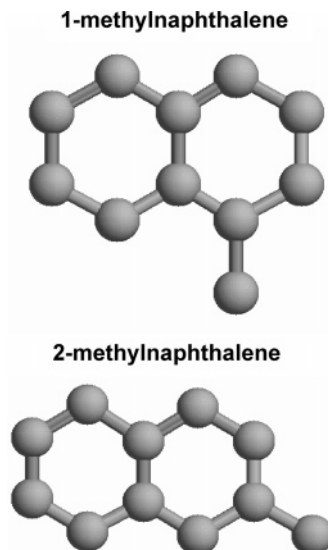


**Figure 1.** Schematic representation of 1- and 2-methylnaphthalene molecules.

**TABLE 1: The LJ Potential Parameters  $\epsilon_i$  and  $\sigma_i$ , Offsets  $\delta_i$ , and Geometries of the 1- and 2-Methylnaphthalene Molecules<sup>17,21,22a</sup>**

group	$\epsilon/k$ (K)	$\sigma$ (Å)	$\delta$ (Å)	C–C bond lengths (Å)
$\text{CH}_3$	120.15	3.6072	0.21584	C– $\text{CH}_3$ : 1.535
CH	89.415	3.2464	0.4071	C–C: 1.40
C	37.726	3.2464	0.0	C–CH: 1.40
				CH–CH: 1.40

<sup>a</sup> Aromatic rings are considered planar with hexagonal symmetry;  $k$  is Boltzmann’s constant.

combining rules.<sup>23</sup> In the present case, the choice of the AUA potential is justified by its very good performance for the thermodynamic properties of naphthalene, in comparison with the common united atom models.<sup>24</sup> The AUA model was also tested for a large variety of aromatic compounds including alkylbenzenes, styrene, triaromatics, and naphthenoaromatics.<sup>17,25</sup>

To model the vapor phase using the B-EOS,  $B$  was determined from a nonproduct algorithm.<sup>26,27</sup> The liquid phase was simulated by canonical molecular dynamics using the Berendsen thermostat<sup>28</sup> to keep the temperature constant. In simulations, we set  $V_1 = 62.45 \text{ nm}^3$  and  $V_2 = 84\,332 \text{ nm}^3$  for 1-methylnaphthalene, and  $V_1 = 61.68 \text{ nm}^3$  and  $V_2 = 74\,567 \text{ nm}^3$  for 2-methylnaphthalene. The total number of particles was  $N = 277$  for 1-methylnaphthalene and  $N = 269$  for 2-methylnaphthalene. A standard cubic simulation box with periodic boundary conditions applied to the center-of-mass (COM) separations was used. The COM cutoff radius was equal to the half-box length. The LJ long-range corrections for  $U$  and  $P$  were included, assuming that the radial distribution functions are unity beyond the COM cutoff radius. The equations of translation and rotational motion were solved by the Gear predictor-corrector algorithm of the fifth and the fourth orders,<sup>23</sup> respectively, with an integration step of 2.5 fs. The coupling time constant  $\tau_T$  in the Berendsen thermostat was set to 0.01 ps. After an equilibration period, simulations were typically performed for 2.5 ns.

To evaluate the probability distribution (see eq 8), the series of  $n_2 V_2 T$  simulations was performed using only a small set of  $n_2$  values at a equidistant spacing; the quantities of interest at intermediate  $n_2$  values were obtained by interpolation. Specifically, we used  $n_2 \in \{256, 260, 264, 268, 272, 276\}$  for

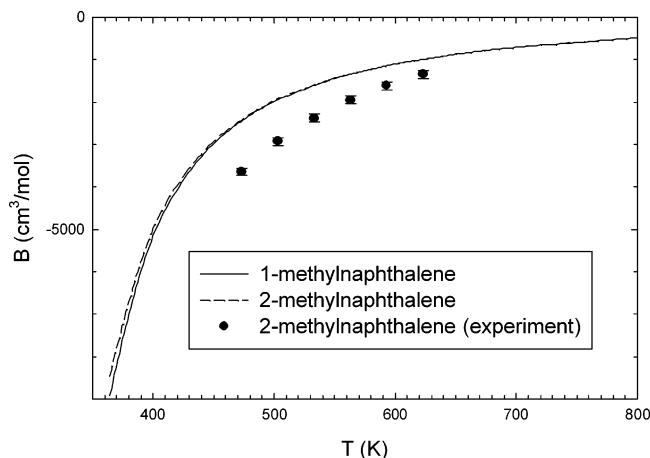


**Figure 2.** The second virial coefficients,  $B$ , of 1- and 2-methylnaphthalene as a function of temperature,  $T$ .

1-methylnaphthalene, and  $n_2 \in \{244, 248, 252, 256, 260, 264, 268\}$  for 2-methylnaphthalene. The TI was performed for  $\lambda = \{0.02, 0.05, 0.1, 0.2, 0.4, 0.6, 0.8, 1.0\}$  using the nonlinear scaling:<sup>29</sup>  $\epsilon$ 's were scaled by  $\lambda$  and  $\sigma$ 's by  $\lambda^{1/3}$  in order to construct a path between the actual state and the ideal gas limit that is free of a phase transition. The interaction between the force centers is then represented by a modified LJ potential

$$u(r_{ab}; \lambda) = 4\epsilon_{ab} \left[ \lambda^5 \left( \frac{\sigma_{ab}}{r_{ab}} \right)^{12} - \lambda^3 \left( \frac{\sigma_{ab}}{r_{ab}} \right)^6 \right] \quad (13)$$

where  $r_{ab}$  is the distance between the force centers  $a$  and  $b$ . The employed nonlinear TI thus scales the repulsion part of the LJ potential by  $\lambda^5$  and the attractive part of the LJ potential by  $\lambda^3$ . Bond lengths and angles were preserved when changing  $\lambda$ .

#### 4. Results and Discussion

Using the numerical and simulation methods explained above, we carried out the required computations at  $T = 364.2$  K.

The second virial coefficient, required in B-EOS, is shown for both compounds in Figure 2 as a function of temperature. The value of  $B$  at the considered temperature,  $T = 364.2$  K, is  $-8912.6$  cm<sup>3</sup>/mol and  $-8457.0$  cm<sup>3</sup>/mol for the 1- and 2-methylnaphthalene, respectively. In the figure, we also show available experimental data<sup>30</sup> (no data seem to be available for 1-methylnaphthalene). Accounting for the fact that the calculated values provide the pure prediction on the basis of the dense liquid-phase properties only, the degree of agreement/disagreement is that one should anticipate.

The key quantity for determining the probability distribution  $P_{N_1, N_2}$  is the change of the internal energy with the coupling parameter  $\lambda$ . A typical dependence of the integrand of eq 9,  $\langle \partial U / \partial \lambda \rangle$ , on  $\lambda$  during the transformation from the liquid phase to an ideal gas is shown in Figure 3. It is worth reminding that the  $\lambda$ -coupling method employed in this work uses an *artificial* path between the actual state and the ideal-gas limit. On the contrary, common TI methods use a *real* path, e.g., along isotherms. Extensive literature dealing with the  $\lambda$ -coupling methods shows that one can construct a path that is free of phase transitions provided that interactions are scaled in a proper way. Consequently, the presence of the kink in the figure does not indicate a phase transition but rather a consequence of the dominance of repulsive interactions over attractive ones when  $\lambda \rightarrow 0$ . Such increase is typically enormous if one uses a linear

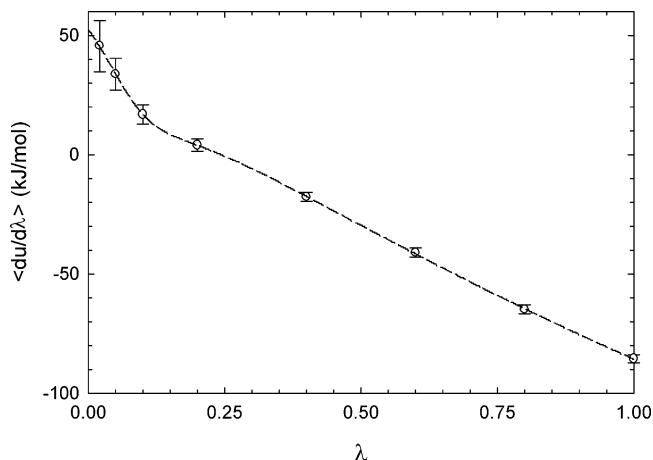


**Figure 3.** The integrand of eq 9,  $\langle \partial U / \partial \lambda \rangle$ , as a function of coupling (scaling) parameter  $\lambda$  during the transformation from the liquid phase to an ideal gas.

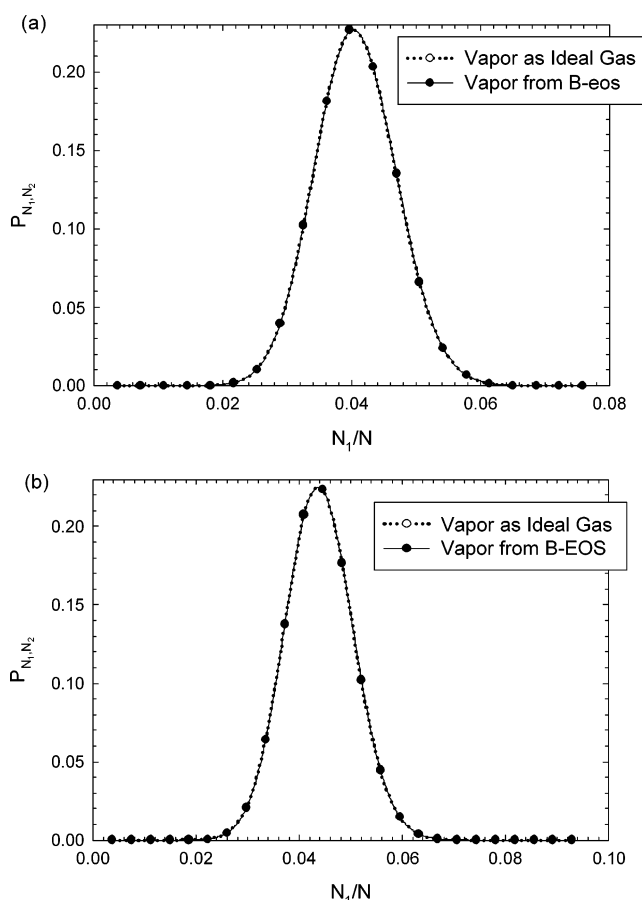


**Figure 4.** The normalized probability distribution,  $P_{N_1, N_2}$ , of the PGE, defined by eq 8, for (a) 1- and (b) 2-methylnaphthalene.

scaling of interactions, but it may be suppressed (but not completely) when employing a nonlinear scaling of interactions as done in this work. As it is seen in Figure 3, the values of  $\langle \partial U / \partial \lambda \rangle$  vary smoothly with  $\lambda$ , which makes it possible to evaluate the integral determining the excess Helmholtz free energy (see eq 9) and, hence, the excess chemical potential, quite accurately. The resulting probability distribution for both compounds is shown in Figure 4. As mentioned above, to estimate the properties of the vapor phase, we used the truncated virial expansion. To assess appropriateness of this approximation, we also treated the vapor phase as an ideal gas. As it is seen from Figure 4, both results are practically indistinguishable.



**TABLE 2: Comparison of the Vapor–Liquid Equilibrium Data Obtained from PGE Simulations for 1- and 2-Methylnaphthalene at  $T = 364.2$  K with GDI Simulations Results<sup>17</sup> and Experimental (DIPPR) Data<sup>31a</sup>**

vapor PGE	1-methylnaphthalene								
	$\rho$ (kg/m <sup>3</sup> )			$\Delta H_{\text{vap}}$ (kJ/mol)			$P_{\text{sat}}$ (kPa)		
	liquid PGE	GDI	expt	PGE	GDI	expt	PGE	GDI	expt
0.031 <sub>2</sub>	1004.7 <sub>23</sub>	1008.7 <sub>29</sub>	967.5	58.6 <sub>5</sub>	59.1 <sub>3</sub>	54.9	0.67 <sub>7</sub>	0.55 <sub>6</sub>	0.62
vapor PGE	2-methylnaphthalene								
	$\rho$ (kg/m <sup>3</sup> )			$\Delta H_{\text{vap}}$ (kJ/mol)			$P_{\text{sat}}$ (kPa)		
	liquid PGE	GDI	expt	PGE	GDI	expt	PGE	GDI	expt
0.037 <sub>2</sub>	984.5 <sub>19</sub>	981.3 <sub>30</sub>	951.9	57.4 <sub>4</sub>	57.1 <sub>2</sub>	55.1	0.80 <sub>7</sub>	0.77 <sub>6</sub>	0.66

<sup>a</sup> (Note that the columns pertaining to the AUA results and experimental data for 1-methylnaphthalene density in Table 5 of ref 17 were erroneously interchanged.)  $\rho$  is the density,  $\Delta H_{\text{vap}}$  is the heat of vaporization, and  $P_{\text{sat}}$  is the vapor pressure. The subscripts denote simulation uncertainties of the last digits.

VLE data obtained from the PGE algorithm using eq 2 are summarized in Table 2. In Table 2, we also provide, for comparison, the simulation results obtained from the GDI method reported in ref 17 and the experimental (DIPPR) data.<sup>31</sup> Heat of vaporization,  $\Delta H_{\text{vap}}$ , was calculated<sup>20</sup> as

$$\Delta H_{\text{vap}} = h_1^{\text{ex}} - h_2^{\text{ex}} \quad (14)$$

where the molar excess enthalpy of the saturated phase  $i$ ,  $h_i^{\text{ex}}$ , is given as

$$h_i^{\text{ex}} = N_A \left[ \frac{U_i^{\text{ex}}}{N_i} + \left( P_{\text{sat}} \frac{V_i}{N_i} - kT \right) \right] \quad (15)$$

In eq 15,  $N_A$  is Avogadro's number and  $P_{\text{sat}}$  is the vapor pressure. We see from Table 2 that the PGE simulation results agree quite well with the GDI simulations results. In each case, the confidence intervals obtained from PGE and GDI are overlapping. This supports the validity of both methods and also the way in which the statistical uncertainties have been estimated. From these comparisons, it seems that the statistical uncertainties are lower than 4 kg/m<sup>3</sup> on liquid density, 0.5 kJ/mol on vaporization enthalpy, and 0.07 kPa on vapor pressure.

In terms of computational efficiency, the proposed PGE method makes it possible to distribute the computation work among parallel processors, each considering different  $\lambda$  and  $n_2$  values. Compared with GDI data based on Monte Carlo methods of ref 17, the number of elementary simulations steps is increased because two parameters,  $\lambda$  and  $n_2$ , have to be varied. In PGE, eight steps were used for  $\lambda$  and six to seven steps for  $n_2$ , so that the total number of elementary simulations steps needed was about 50. In the GDI, three GE simulations were employed at temperatures above 500 K, and four NPT simulations of the liquid phase were used between 364 and 500 K, so that the total of seven simulations were required. However, longer simulations were required for the GDI to reach the same accuracy as in PGE. Also, each elementary simulation involved in PGE, being performed through molecular dynamics, could be parallelized more efficiently than Monte Carlo methods used in the GDI of ref 17. Another point to mention is that GDI provides the equilibrium properties for the temperature range considered, while PGE provides them for a single temperature.

In terms of force field validation, we observe first that liquid densities and heats of vaporization are overestimated, and this is typical for uncertainties one may encounter when using a general force field. Nevertheless, the accuracy of 1- and 2-methylnaphthalene simulation results allows us to evaluate precisely the influence of the methyl group location. The

predicted liquid density for 1-methylnaphthalene is about 17–20 kg/m<sup>3</sup> higher, while experimental data indicate it should be about 16 kg/m<sup>3</sup> higher. Considering that the maximum uncertainty of the DIPPR correlations is approximately 8 kg/m<sup>3</sup>, it is clear that the density difference between both isomers is correctly predicted. This density difference may be attributed to the slightly lower volume of the 1-methylnaphthalene molecule because the excluded volume by the methyl group has a larger overlap with the aromatic rings than in 2-methylnaphthalene. The predicted difference in vaporization enthalpy between both isomers is about 1.4–2 kJ/mol, while it is 0.2 kJ/mol if we follow the DIPPR correlations. However, the uncertainty of vaporization enthalpy correlations from DIPPR is rather large, as maximum deviations reach 2.6%, i.e., 1.4 kJ/mol. Also, it is known that, for high-molecular-weight compounds, heats of vaporization are often derived from vapor pressures through the Clapeyron equation, and this indirect way of measurement probably contributes to increased uncertainties. Simulation results are logical, as a higher density is expected to correspond to a higher heat of vaporization (this is basically due to increased number of force center pairs located within the range of the interaction potential). We may thus argue that simulation results might be qualitatively more correct concerning assessment of the influence of methyl group position on vaporization enthalpy. From PGE and GDI simulations, we get that the vapor pressure of 1-methylnaphthalene is lower by 0.1 to 0.22 kPa (i.e., from 13 to 29%), whereas the DIPPR correlations state, it is 10% lower. Although there is a substantial uncertainty in DIPPR correlations for this property (maximum deviations with raw data reach up to 20%), the lower vapor pressure of 1-methylnaphthalene is consistent with its measured normal boiling point, which is by 3.5 K lower than that of 2-methylnaphthalene. Here again, there is thus a fair agreement between the predicted influence of the location of the methyl group and experimental data.

## 5. Conclusions

In the present work, we have implemented the parallelized version of the Gibbs ensemble (PGE) method in order to assess its efficiency when determination of phase equilibria of complex compounds of industrial interest are required. The idea behind this parallelization is to bypass the physical transfer of complex molecules between boxes representing different phases by computing the chemical potential in a canonical ensemble for which a number of sophisticated methods have been developed. For this purpose, we used in this paper the thermodynamic integration ( $\lambda$ -coupling) technique. Although this technique has been here applied to rigid molecules, it is worth mentioning

that, with respect to potential future applications, it is also applicable to flexible molecules.

The PGE method has been designed for conditions at which the conventional GE simulation fails. We have therefore compared the considered PGE method with available low temperature data reported in ref 17 and obtained using the GDI integration based on Monte Carlo methods that seems the only reasonable alternative for the problem at hand. Just from the computational point of view, both methods seem, roughly, equivalent. From the point of applications, there is however a substantial advantage of the proposed method: it involves molecular dynamics simulations, while the implementation of the GDI method used in ref 17 employs Monte Carlo methods that are less routinely available for heavy molecules. Moreover, each molecular dynamics simulations can further be parallelized more efficiently and straightforwardly than the Monte Carlo simulations used in the GDI.

Concerning a secondary goal of this research, validation of the available force fields, the present study confirms a fair agreement between measured and predicted properties of 1- and 2-methynaphthalene. More importantly, it establishes more firmly that the influence of the position of the methyl group on the saturated liquid density is correctly predicted. This effect could be related to the difference in molecular volume between the isomers. The influence on saturation pressure and vaporization enthalpy appears also well described, but these properties are subject to higher simulation or experimental uncertainties.

**Acknowledgment.** This research was supported by the Czech National Research Program "Information Society" (project 1ET400720409). Travel support under the CNRS/ASCR bilateral agreement is also acknowledged.

## References and Notes

- (1) Panagiotopoulos, A. Z. *Mol. Phys.* **1987**, *61*, 813.
- (2) Mecke, M.; Winkelmann, J.; Fischer, J. *J. Chem. Phys.* **1997**, *107*, 9264.
- (3) Nezbeda, I.; Kolafa, J. *Mol. Simul.* **1991**, *5*, 391.
- (4) Lyubartsev, A. P.; Martsinovskii, A. A.; Shevkunov, S. V.; Vorontsov-Velyaminov, P. N. *J. Chem. Phys.* **1992**, *96*, 1776.
- (5) Frenkel, D.; Smit, B. *Understanding Molecular Simulation: From Algorithms to Applications*; Academic Press: London, 2002.
- (6) Lu, N.; Kofke, D. A. *J. Chem. Phys.* **1999**, *111*, 4414.
- (7) Lu, N.; Singh, J. K.; Kofke, D. A. *J. Chem. Phys.* **2003**, *118*, 2977.
- (8) Esselink, K.; Loyens, L. D. J. C.; Smit, B. *Phys. Rev. E* **2005**, *51*, 1560.
- (9) Loyens, L. D. J. C.; Smit, B.; Esselink, K. *Mol. Phys.* **1995**, *86*, 171.
- (10) Shi, W.; Johnson, J. K. *Fluid Phase Equilib.* **2001**, *187–188*, 171.
- (11) Errington, J. R.; Panagiotopoulos, A. Z. *J. Chem. Phys.* **1998**, *109*, 1093.
- (12) Potoff, J. J.; Panagiotopoulos, A. Z. *J. Chem. Phys.* **1998**, *109*, 10914.
- (13) Kofke, D. A. *J. Chem. Phys.* **1993**, *98*, 4149.
- (14) Shing, K. S.; Azadipour, S. R. *Chem. Phys. Lett.* **1992**, *190*, 386.
- (15) Vega, L. F.; Shing, K. S.; Rull, L. F. *Mol. Phys.* **1994**, *82*, 439.
- (16) Strnad, M.; Nezbeda, I. *Mol. Phys.* **2000**, *98*, 1887.
- (17) Ahunbay, M. G.; Perez-Pellitero, J.; Contreras-Camacho, R. O.; Teuler, J.-M.; Ungerer, P.; Mackie, A. D.; Lachet, V. *J. Phys. Chem. B* **2005**, *109*, 2970.
- (18) Panagiotopoulos, A. Z. *Mol. Simul.* **1992**, *9*, 1.
- (19) Smit, B.; Frenkel, D. *Mol. Phys.* **1989**, *68*, 951.
- (20) Poling, B. E.; Prausnitz, J. M.; O'Connell, J. P. *The Properties of Gases and Liquids*; McGraw-Hill: New York, 2000.
- (21) Ungerer, P.; Beauvais, Ch.; Delhommelle, J.; Boutin, A.; Rousseau, B.; Fuchs, A. H. *J. Chem. Phys.* **2000**, *112*, 5499.
- (22) Contreras-Camacho, R. O.; Ungerer, P.; Boutin, A.; Mackie, A. D. *J. Phys. Chem. B* **2004**, *108*, 14109.
- (23) Allen, M. P.; Tildesley, D. J. *Computer Simulation of Liquids*; Clarendon Press: Oxford, 1987.
- (24) Wick, C. D.; Martin, M. G.; Siepmann, J. I. *J. Phys. Chem B* **2000**, *104*, 8008.
- (25) Ahunbay, M. G.; Kranias, S.; Lachet, V.; Ungerer, P. *Fluid Phase Equilib.* **2004**, *224*, 73.
- (26) Stroud, A. H. *Approximate Calculation of Multiple Integrals*; Prentice Hall: New York, 1971.
- (27) Murad, S. *Linear and Nonlinear Quantum Chemistry Program Exchange*; QCPE 12:357; Indiana University: Bloomington, IN, 1978.
- (28) Berendsen, H. J. C.; Postma, J. P. M.; van Gunsteren, W. F.; DiNola, A.; Haak, J. R. *J. Chem. Phys.* **1984**, *81*, 3684.
- (29) Tironi, I. G.; van Gunsteren, W. F. *Mol. Phys.* **1994**, *83*, 381.
- (30) Dymond, J. H.; Marsh, K. N.; Wilhoit, R. C.; Wong, K. C. *The Virial Coefficients of Pure Gases and Mixtures*; Springer-Verlag: Berlin, 2002.
- (31) Rowley, R. L.; Wilding, W. V.; Oscarson, J. L.; Zundel, N. A.; Marshall, T. L.; Daubert, T. E.; Danner, R. P. *DIPPR Data Compilation of Pure Compound Properties*; Design Institute for Physical Properties, AIChE: New York, 2002.